# Influence of Ordered Morphology on the Anisotropic Actuation in Uniaxially Oriented Electroactive Polymer Systems

**Jong Keun Park and Robert B. Moore***

Macromolecules and Interfaces Institute, Department of Chemistry, Virginia Polytechnic Institute and State University, Blacksburg, Virginia 24061

**ABSTRACT** Ionic polymer−metal composites (IPMCs) are electroactive materials that undergo bending motions with the stimulus of a relatively weak electric field. To understand the fundamental role of the nanoscale morphology of the ionomer membrane matrix in affecting the actuation behavior of IPMC systems, we evaluated the actuation performance of IPMC materials subjected to uniaxial orientation. The perfluorinated ionomer nanostructure altered by uniaxial orientation mimicks the fibrillar structure of biological muscle tissue and yields a new anisotropic actuation response. It is evident that IPMCs cut from films oriented *perpendicular* to the draw direction yield tip-displacement values that are significantly *greater* than those of unoriented IPMCs. In contrast, IPMCs cut from films oriented *parallel* to the draw direction appear to resist bending and yield tip-displacement values that are *much less* than those of unoriented IPMCs. This anisotropic actuation behavior is attributed, in part, to the contribution of the fibrillar morphology to the bulk bending modulus. As an additional contribution, electrically stimulated water swelling perpendicular to the rodlike aggregate axis facilitates bending in the perpendicular direction.

**KEYWORDS:** electroactive polymer (EAP) • ionic polymer−metal composite (IPMC) • orientation of ionomers • Nafion • membrane

## INTRODUCTION

Electroactive polymers (EAPs) respond to electrical stimulation with a significant change in their size or shape and have therefore recently attracted increasing interest with the potential for technologically important applications ranging from biologically inspired artificial muscles to micro/nanofluidics and robotics (1). Various types of polymers have been considered as electroactive materials, including conducting polymers (2, 3), dielectric elastomers (4), polymer gels (5), and ionic polymer−metal composites (IPMCs) (6−9).

Among EAPs, IPMCs are considered as one of the most promising candidates for artificial muscles because of their capability of significant mechanical motion with the stimulus of a relatively weak electric field (e.g., 1−5 V) (8). Conversely, an external mechanical force applied to the surface of an IPMC can stimulate a detectable electrical response, and thus the system acts as a motion sensor. IPMCs are typically fabricated through electroless deposition of a conductive metal (e.g., platinum or gold) onto both surfaces of an ion-exchange membrane (6). The standard electroding procedure involves neutralization of an ionomer with relatively bulky metal ions, such as $Pt^{II}$. Subsequently, the ionomer membrane is dipped into an aqueous reducing agent (e.g., $NaBH_4$) to convert the $Pt^{II}$ ions to Pt metal. Because of the "outside-in" diffusion of the reducing agent and the inside-out diffusion of the $Pt^{II}$ ions, Pt nanoparticles are nucleated and grow near the surfaces of the membrane. With sufficient amounts of Pt metal, the surfaces become electrically conductive, thus forming the IPMC electrode layers.

A review of the open literature reveals that the vast majority of previous IPMC studies have principally involved a perfluorosulfonate ionomer (PFSI), Nafion, in a single morphological state (i.e., as-received membranes supplied by DuPont). Nafion is a copolymer of tetrafluoroethylene and generally less than 15 mol % of perfluorovinyl ether units terminated with sulfonic acid functionalities (10). Thus, with this commercially available Nafion platform, only one structure has been evaluated and, consequently, only a limited set of actuation properties have been observed. In order to expand these structure−property relationships, we have previously demonstrated many ways to manipulate morphology in PFSIs (11−13). By recognizing the existence of rodlike aggregates within Nafion (10, 14, 15), we have subjected Nafion films to uniaxial orientation to create an anisotropic fibrillar morphology. The resulting, hierarchical structure mimicks natural muscle tissue, which is also highly anisotropic in nature. By understanding the fundamental role of the nanoscale morphology of the ionomer membrane in affecting the actuation behavior of IPMC systems, we hope to gain a unique insight into the molecular-level processes associated with the, as of yet, unexplained IPMC actuation mechanism. Moreover, this knowledge will foster the development of tailored processing procedures for ionic polymer membranes in the design of the next-generation platform for electroactive materials.

* E-mail: rbmoore3@vt.edu.
Received for review December 10, 2008 and accepted February 16, 2009
DOI: 10.1021/am8002268

## EXPERIMENTAL SECTION

**Materials.** Extruded Nafion 117 from E.I. DuPont de Nemours & Co. (1100 g equiv$^{-1}$, sulfonic acid form) was precleaned by refluxing in 8 M nitric acid for 2 h and then in deionized (DI) water for 1 h. Tetrabutylammonium ($TBA^+$)-neutralized membranes were prepared by soaking the cleaned $H^+$-form membranes in tetrabutylammonium hydroxide (TBAOH; Aldrich) in methanol solutions (1 M) for 12 h and then rinsing with methanol to remove the residual TBAOH. This rinse consisted of three wash cycles in 200 mL of methanol under ultrasonic agitation. These neutralized membranes were then dried at 70 °C overnight in a vacuum oven.

**Fabrication of Oriented IPMC.** Uniaxially oriented samples of Nafion were prepared by cutting the $TBA^+$-neutralized membranes into dog-bone shapes and mounting them on a specially designed drawing apparatus. This drawing apparatus allowed $TBA^+$-neutralized Nafion membranes to be drawn at 90 °C to a draw ratio [$\lambda$ = final length ($L$)/initial length ($L_0$)] of 2 as determined by the displacement of ink marks on the samples. Uniaxially oriented $TBA^+$-form membranes were then mounted in Kel-F clamps and converted to the $H^+$ form by boiling in 4 M $H_2SO_4$/MeOH for 1 h, in MeOH for 30 min, and in DI water for 30 min. These oriented $H^+$-form Nafion samples were then used to fabricate oriented IPMCs following the standard multistep electroding procedure after surface roughening by mechanically rubbing the surface with 400-grain sandpaper (6). A platinum salt complex $[Pt(NH_3)_4]Cl_2$ (Aldrich) was used to make an aqueous solution with a concentration of 2 mg mL$^{-1}$. The $H^+$-form Nafion membrane was allowed to equilibrate with the platinum salt solution overnight. After rinsing with DI water, the membrane was immersed in DI water and the $Pt^{II}$ ions in the membrane were reduced to Pt metal particles using 5 wt % aqueous sodium borohydride ($NaBH_4$; Aldrich). The addition of $NaBH_4$ was carried out in seven steps at 30 min intervals, over which the temperature was ramped from 40 to 60 °C. After completion of the initial series of $NaBH_4$ additions, a final addition was performed and reduction was allowed to proceed for 1.5 h. The electroded membrane was then rinsed in water before immersion in 0.1 M HCl to convert the material to the acid form. The whole reduction process above was carried out for three cycles to produce the final IPMCs used in the current study. Following the complete electroding procedure, the oriented IPMCs were removed from the Kel-F clamps and were observed to be dimensionally stable, with a swollen thickness of 200 $\mu$m.

**Fabrication of Unoriented IPMC.** $TBA^+$-form Nafion was converted to $H^+$ form by boiling in 4 M $H_2SO_4$/MeOH for 1 h, in MeOH for 30 min, and in DI water for 30 min. Ion-exchange processes from $H^+$ to $TBA^+$ and then back to $H^+$ form are necessary in terms of membrane initialization protocol to ensure that unoriented IPMCs entered experimentation in the same chemical state and experienced the same swelling and thermal histories as those of oriented IPMCs. These control $H^+$-form Nafion membranes were used to fabricate the unoriented IPMCs following the standard multistep electroding procedure described above. The swollen thickness of the unoriented IPMC was measured to be 230 $\mu$m.

**Small/Wide-Angle X-ray Scattering (SAXS/WAXS).** SAXS and WAXS images were acquired at the Advanced Photon Source, Argonne National Laboratory (Beamline 5-ID DND-CAT). The wavelength of the X-ray beam was 0.8266 Å, and the sample-to-detector distances for SAXS and WAXS were 1343 and 228 mm, respectively. SAXS and WAXS two-dimensional images were simultaneously obtained using a Mar CCD and Roper camera, respectively, with a 5 s exposure time.

**Measurement of Tip Displacement.** Characterization of the actuation performance was carried out using a LabView-based system devised in-house. Square-waveform input signals were generated using a Function Generator VI (LabView) and sent to an external amplifier using a DAQ card (National Instruments PCI-6024E). All samples were cut to 2.0 cm in length and 0.5 cm in width and fully hydrated before any measurement. Displacement of the IPMCs under different electrical stimuli was captured by means of an Imaging Solutions Group camera (LightWise LW-1.3-R-1394) interfaced to LabView. Final image analysis was accomplished using *Datapoint* software (Xannah Applied Science and Engineering).

**Determination of the Bending Modulus.** The bending moduli of unoriented/oriented $TBA^+$-form Nafion and hydrated $H^+$-form IPMCs were measured by dynamic mechanical analysis performed on a TA Intruments (DMA Q800 analyzer) in the bending mode using a micro-three-point bending clamp. All of the measurements were conducted at room temperature with the furnace open. An applied strain of 0.5% and four different frequencies, 0.1, 0.5, 1.0, and 10 Hz, were investigated.

**TEM Characterization of the IPMC Cross Section.** Transmission electron microscopy (TEM) was used for the nanoscale characterization of IPMC morphology (including Pt nanoparticle size, shape, and spatial distribution) in unoriented and oriented IPMCs. TEM micrographs of IPMC cross sections were obtained using a JEOL JEM-2100 LaB6 microscope operated at 200 keV. IPMC samples were first embedded in an epoxy resin, and microtomed sections (thickness 100 nm) were deposited on a carbon-coated copper grid.

## RESULTS AND DISCUSSION

With a sufficient length of poly(tetrafluoroethylene) (PTFE) segments between side chains, Nafion is capable of organizing into crystalline domains (generally less than ca. 10 wt % in 1100 equiv wt of Nafion). Greater efforts, however, have been given to the unique nanophase-separated morphology observed upon aggregation of the polar, ionic side chains within the matrix of hydrophobic PTFE. These ionic clusters, and specifically their spatial distribution and connectivity, precisely define the supramolecular organization and function of this technologically important material as an ionic conductor. It has also been shown that these ionic aggregates act as multifunctional physical cross-links that significantly restrict chain mobility (12, 16). In an effort to increase the melt-flow character of Nafion, Moore and Cable utilized large, hydrophobic $TBA^+$ counterions to effectively diminish the strength of Coloumbic interactions within the ionic domains (12, 13, 17, 18). This approach profoundly increased the ability to uniaxially orient Nafion up to draw ratios ($\lambda = L/L_0$) of about 6 (13, 19). The consequence of this orientation has been characterized in terms of anisotropic morphologies (13, 15, 19−24) and ionic conductivities (13), indicating a strong alignment of ionic domains along the stretching direction. However, no study has been reported that exploits the significance of this morphological orientation on the actuation behavior in IPMCs.

The effects of uniaxial deformation on the morphology of $TBA^+$-form Nafion have been characterized by two-dimensional SAXS/WAXS. For the as-received state (Figure 1a), the relatively (25) isotropic SAXS data show a diffuse outer ring of maximum intensity at ca. $q = 0.1-0.2$ Å$^{-1}$, which has been attributed to scattering from the ionic aggregates dispersed in the PTFE matrix (10, 18−21). The intense scattering near the beam stop is associated with typical ionomer long-range heterogeneities (16, 26) and a contribution from PTFE-like crystalline domains (14, 18,

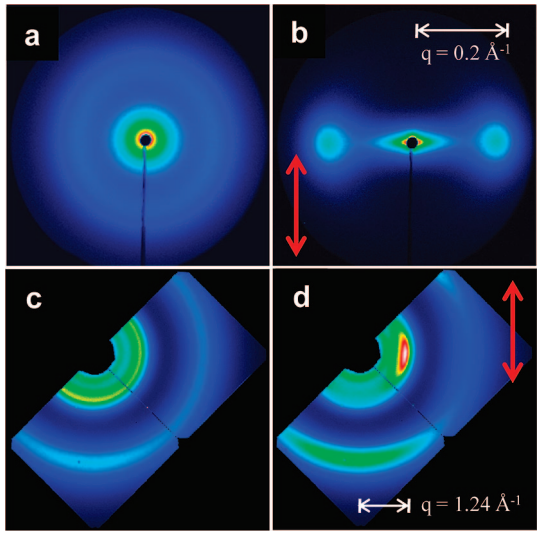


**FIGURE 1. Two-dimensional X-ray scattering patterns of $TBA^+$-form Nafion: (a) SAXS of unoriented and (b) uniaxially oriented ($\lambda = 2$) samples and (c) WAXS of unoriented and (d) uniaxially oriented samples. Stretching directions are indicated with red arrows.**

20, 21). As the film is stretched to a draw ratio, $\lambda = 2$, the previously isotropic scattering profile transforms into a strongly anisotropic scattering pattern (i.e., equatorial spots), as is clearly observed in Figure 1b. van der Heijden and coworkers attributed this anisotropic scattering to the alignment of elongated polymeric aggregates in the direction of uniaxial extension (15). With further extension, equatorial streaking in the SAXS patterns is observed, consistent with the formation of fibrillar-like morphologies (10, 13, 19).

In the unoriented WAXS image (Figure 1c), two rings can be observed, where the inner ring is attributed to the weak reflection of PTFE-like crystallites, $hkl = 100$ at $q = 1.24$ Å$^{-1}$ (27), which is superimposed as a shoulder on a broad amorphous halo. The outer ring in Figure 1c is attributed to the PTFE crystalline reflection $hkl = 101$ at $q = 2.72$ Å$^{-1}$ (27). For the oriented sample, anisotropic WAXS patterns (i.e., equatorial arcs) indicate that both the amorphous and crystalline chains are oriented parallel to the direction of stretching, as shown in Figure 1d (15). These chain orientations are consistent with a fibrillar morphology and the alignment of rodlike ionic domains in the stretching direction.

Once Nafion membranes are uniaxially oriented, electroless plating of platinum was performed following a multistep procedure to prepare the nanostructured electrode layers (consisting of densely packed Pt nanoparticles) of the IPMC (6). With a 3 V square-waveform stimulus (i.e., a field strength of ca. 15 V mm$^{-1}$), these IPMCs display significant bending actuation, as shown in the overlay images of Figure 2. For the oriented IPMCs, the actuation behavior is clearly anisotropic and differs greatly in amplitude from that of the unoriented sample. It is evident that IPMCs cut from films oriented perpendicular to the draw direction (Figure 2d) yield tip-displacement values that are significantly greater than those of unoriented IPMCs (Figure 2a). In contrast, IPMCs cut from films oriented parallel to the draw direction (Figure 2c) appear to resist bending and yield tip-displacement values that are much less than those of unoriented IPMCs.

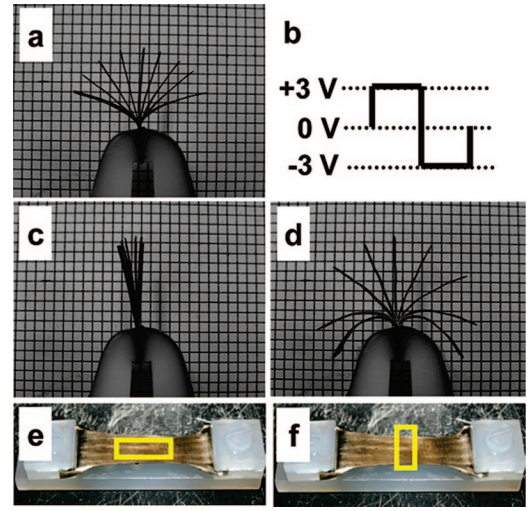


**FIGURE 2. Composite overlay of images (square-grid dimensions of 2 mm) captured during bending actuation of (a) unoriented IPMCs, oriented IPMCs cut (c) parallel and (d) perpendicular to the draw direction under (b) 3 V square-waveform input with a frequency of 0.1 Hz. As-fabricated oriented IPMC with a rectangular box indicating the direction of sample orientation, (e) parallel and (f) perpendicular to draw direction.**

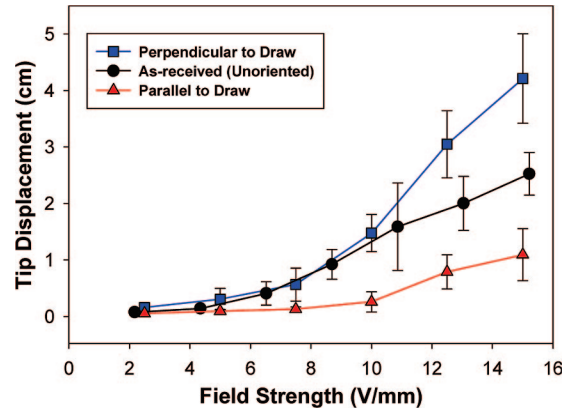


**FIGURE 3. Plot of tip displacement versus field strength (defined as the applied voltage divided by the IPMC thickness). All samples were 2 cm in length and 5 mm in width. Error bars are the result of repetitive sample preparation under identical orientation and electroding conditions.**

As a quantitative measure of this actuation performance, Figure 3 shows plots of tip displacement versus field strength (the applied voltage divided by the IPMC thickness). At relatively low field strengths (below 6 V mm$^{-1}$), the electrically stimulated driving force for actuation (7, 28, 29) is inadequate to cause significant bending motion. Upon application of higher field strengths, the tip displacement for each IPMC increases significantly. Moreover, at field strengths above 10 V mm$^{-1}$, the anisotropic actuation in these oriented IPMCs is well resolved (i.e., perpendicular is more responsive than parallel) and becomes much more evident with increasing field strength. At 15 V mm$^{-1}$, the perpendicular IPMC yields a tip displacement that is 2 times that of the unoriented system and 4 times that of the parallel IPMC.

Because of precise morphological control with uniaxial extension (shown above), we have also observed that samples cut 45° to the draw direction (Figure 4) yield a never before

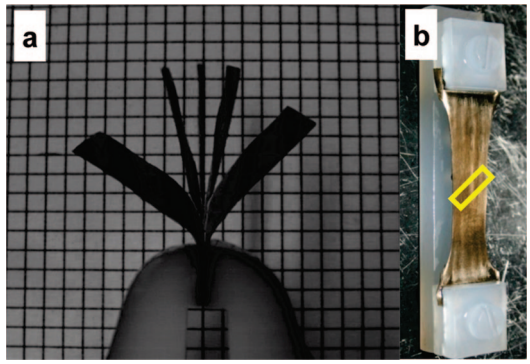


FIGURE 4. (a) Composite overlay of images (square-grid dimensions of 2 mm) captured during twisting actuation of IPMCs cut 45° to the draw direction under 2.5 V square-waveform input with a frequency of 0.1 Hz. (b) As-fabricated oriented IPMC with a rectangular box indicating the direction of sample orientation, 45° to the draw direction.

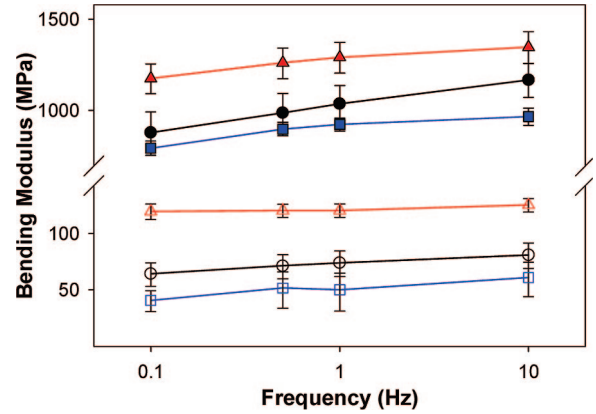


FIGURE 5. Effects of uniaxial orientation on the bending moduli of the ionic polymer matrix. Dry, $TBA^+$-form Nafion bent along the draw direction (filled triangles), unoriented (filled circles), and bent across the draw direction (filled squares); water-swollen, $H^+$-form IPMC bent along the draw direction (open triangles), unoriented (open circles), and bent across the draw direction (open squares).

seen twisting mode of actuation for these "bending actuators". While this unique observation may open many new applications for these composite systems, it is of fundamental importance to recognize that these data show, for the first time, the impact of ionomer morphology on the actuation behavior. Moreover, physical models developed to explain the actuation response of IPMCs must now consider the contribution of this structural parameter to the overall actuation mechanism.

Mechanisms for the bending actuation in IPMCs have been suggested to involve an electrically stimulated differential swelling across the membrane thickness (7) or changes in the dimensional symmetry of the water-swollen clusters due to local electrostatic polarization (29). In order to investigate the true mechanism of IPMC actuation, we have recently initiated neutron imaging studies to probe the existence and role of water and ion gradients during the actuation response (30). Despite the lack of a precise, molecular-level understanding of the actuation mechanism, it is clear that the driving force for actuation must overcome the intrinsic stiffness of the bulk actuator. Specifically, the induced curvature in these bending actuators is inversely proportional to the bulk modulus of the IPMC (28). To explore the effects of uniaxial orientation on the bending stiffness of the ionic polymer matrix, we employed dynamic mechanical analysis using a three-point bending clamp. Figure 5 shows the measured bending moduli of a dry, $TBA^+$-form Nafion membrane (without electrode layers) and a hydrated, $H^+$-form IPMC (with electrode layers) at frequencies ranging from 0.1 to 10 Hz. The dry ionomer samples are observed to yield bending moduli that are an order of magnitude higher than that of the hydrated IPMC. This behavior is attributed to water acting as a softening (plasticizing) agent in the swollen IPMC. In complete agreement with the anisotropic actuation behavior, both samples demonstrate that bending *along* the draw direction (parallel orientation) yields a higher modulus value relative to the unoriented state. In contrast, bending *across* the draw direction (perpendicular orientation) yields a lower modulus value relative to the unoriented state. It is important to note from this comparison that the observed anisotropy in bending moduli is attributed to the oriented state of the ionic polymer and is not affected by the electroding process.

On the basis of our X-ray results (Figure 1), the increased moduli of the oriented films along the draw direction may be attributed to the oriented morphology of the ionic polymer matrix, including the alignment of polymer chains, crystallites, and ionic domains. This is not surprising given the inherent stiffness of the PTFE segments of the Nafion backbone (31, 32). Furthermore, it is reasonable to expect that the water-swollen, rodlike ionic aggregates (24) act as nanoscale, anisotropic fillers in the matrix and resist folding along the aggregate axis. Consequently, this oriented morphology leads to anisotropic actuation. Because the oriented IPMCs are stiffer along the draw direction, actuation upon electrical stimulation is inhibited. Conversely, the lower bending modulus of IPMCs oriented perpendicular to the draw direction yields enhanced actuation.

It is of interest to note that anisotropy in actuation strain due to chain alignment has been observed recently in conducting polymer systems (3). For these EAPs, anisotropy was attributed to the migration of counterions to locations between the oriented polymer chains, which yielded a higher degree of swelling perpendicular to the chain axis (3). A similar swelling mechanism (i.e., water swelling perpendicular to the rodlike aggregate axis) may be envisioned for the oriented IPMC system studied here. For example, bulk water swelling of the unoriented ionomer shows an isotropic increase in the dimensions of ca. 25%. In contrast, the oriented ionomer shows a negligible swelling along the draw direction, with an enhanced swelling of ca. 40% in the perpendicular directions. Because swelling along the aggregate length is inhibited because of morphological stability, preferential swelling in the perpendicular directions facilitates the observed anisotropy in actuation. However, the contributions of the stiff PTFE chains and oriented crystallites are also likely to be contributing factors. Therefore, the anisotropic actuation observed in these oriented IPMCs demonstrates, for the first time, the important contribution

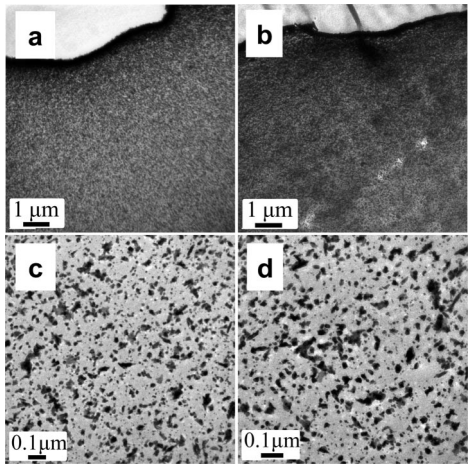


**FIGURE 6. TEM micrographs of unoriented IPMCs at low (a) and high (c) magnifications and oriented IPMCs at low (b) and high (d) magnifications.**

of the ionomer membrane morphology and chain conformation in the overall actuation phenomenon.

While the structural parameters of the ionic polymer matrix are now shown to be important contributions in the overall actuation mechanism, the effect of matrix orientation on the Pt nanoparticle formation and distribution within the electrode layers should also be considered as contributing factors. TEM micrographs of both unoriented (Figure 6a) and oriented (Figure 6b) IPMCs allow the investigation of Pt particle distribution within these Nafion membranes. Both images display very thin dense layers (ca. 0.5 $\mu$m) of Pt particles at the film edge and less densely dispersed Pt particles toward the film interior. While not shown in these images, the Pt particles in IPMCs are essentially absent at a depth beyond ca. 30 $\mu$m from the membrane surface. TEM micrographs of higher magnifications of both unoriented (Figure 6c) and oriented (Figure 6d) IPMCs show essentially no difference regarding the spatial distribution, average size, and shape of the Pt particles, implying that uniaxial stretching has no significant effect on Pt particle formation. On the other hand, orientation yields a profound reorganization of the nanoscale morphology of the matrix, as shown in the two-dimensional X-ray scattering patterns (Figure 1). From this information, it is evident that the Pt particle morphology/size or shape has no impact on the observed anisotropic actuation, thus supporting our argument that the actuation response is attributable to the oriented morphology of the ionic polymer matrix.

## CONCLUSION

Uniaxial orientation of Nafion and the subsequent formation of electrode layers to create an IPMC were observed to yield anisotropic actuation behavior upon electrical stimulation. Relative to the unoriented state, polymer chains, crystallites, and rodlike aggregates oriented parallel to the draw direction inhibit actuation in the parallel orientation, while bending in the perpendicular orientation is significantly enhanced. In line with this unique anisotropic actuation behavior, dynamic mechanical analysis also showed that bending across the draw direction (perpendicular orientation) yields a lower modulus value relative to the unoriented state and a value much lower relative to bending along the draw direction (parallel orientation). Thus, the anisotropic actuation behavior of these oriented IPMCs is attributed, in part, to the contribution of the nanoscale morphology to the bulk bending modulus. As an additional contribution, electrically stimulated water swelling perpendicular to the rodlike aggregate axis facilitates bending in the perpendicular direction. Overall, this study clearly demonstrates, for the first time, the importance of the nanoscale morphology in affecting/controlling the actuation behavior in IPMC electroactive systems. Further work is underway to investigate the effects of the draw ratio, draw rate, and draw temperature for the purpose of performance optimization.

**Acknowledgment.** The authors acknowledge support for this work provided by the National Science Foundation (Grants CMMI-0707364 and CBET-0756439) and the Materials Research Science and Engineering Center (MRSEC) program at the University of Southern Mississippi (Grant DMR-0213883). Use of the Advanced Photon Source was supported by the U.S. Department of Energy, Office of Science, Office of Basic Energy Sciences, under Contract DE-AC02-06CH11357.

## REFERENCES AND NOTES

(1) Bar-Cohen, Y. EAP History Current Status, and Infrastructure. In *Electroactive Polymer (EAP) Actuators as Artificial Muscles*; Bar-Cohen, Y., Ed.; SPIE: Bellingham, WA, 2001; pp 3–44.
(2) Smela, E. *Adv. Mater.* **2003**, *15*, 481–494.
(3) Pytel, R.; Thomas, E.; Hunter, I. *Chem. Mater.* **2006**, *18*, 861–863.
(4) Pelrine, R.; Kornbluh, R.; Pei, Q.; Joseph, J. *Science* **2000**, *287*, 836–839.
(5) Liu, Z.; Calvert, P. Multilayer Hydrogels as Muscle-Like Actuators. *Adv. Mater.* **2000**, *12*, 288–291.
(6) Shahinpoor, M.; Kim, K. J. *Smart Mater. Struct.* **2001**, *10*, 819–833.
(7) Shahinpoor, M. *Electrochim. Acta* **2003**, *48*, 2343–2353.
(8) Duncan, A. J.; Leo, D. J.; Long, T. E. *Macromolecules* **2008**, *41*, 7765–7775.
(9) Nemat-Nasser, S.; Wu, Y. *Smart Mater. Struct.* **2006**, *15*, 909–923.
(10) Mauritz, K. A.; Moore, R. B. *Chem. Rev.* **2004**, *104*, 4535–4585.
(11) Moore, R. B.; Martin, C. R. *Macromolecules* **1988**, *21* (5), 1334–1339.
(12) Moore, R. B.; Cable, K. M.; Croley, T. L. *J. Membr. Sci.* **1992**, *75*, 7–14.
(13) Cable, K. M.; Mauritz, K. A.; Moore, R. B. *Chem. Mater.* **1995**, *7*, 1601–1603.
(14) Rubatat, L.; Rollet, A. L.; Gebel, G.; Diat, O. *Macromolecules* **2002**, *35*, 4050–4055.
(15) van der Heijden, P. C.; Rubatat, L.; Diat, O. *Macromolecules* **2004**, *37*, 5327–5336.
(16) Eisenberg, A.; Hird, B.; Moore, R. B. *Macromolecules* **1990**, *23*, 4098–4107.
(17) Page, K. A.; Jarrett, W.; Moore, R. B. *J. Polym. Sci., Part B: Polym. Phys.* **2007**, *45*, 2177–2186.
(18) Page, K. A.; Cable, K. M.; Moore, R. B. *Macromolecules* **2005**, *38*, 6472–6484.
(19) Page, K. A.; Landis, F. A.; Phillips, A. K.; Moore, R. B. *Macromolecules* **2006**, *39*, 3939–3946.
(20) Gierke, T. D.; Munn, G. E.; Wilson, F. C. *J. Polym. Sci., Polym. Phys. Ed.* **1981**, *19*, 1687–1704.
(21) Fujimura, M.; Hashimoto, T.; Kawai, H. *Macromolecules* **1982**, *15*, 136–144.
(22) Elliott, J. A.; Hanna, S. *Macromolecules* **2000**, *33*, 4161–4171.
(23) Londono, J. D.; Davidson, R. V.; Mazur, S. *Polym. Mater.: Sci. Eng.* **2001**, *85*, 23–24.
(24) Schmidt-Rohr, K.; Chen, Q. *Nat. Mater.* **2008**, *7*, 75–83.

(25) Small intrinsic orientational anisotropy in the as-received state is attributed to the melt-extrusion process through a die used to produce the membranes (i.e., machine direction).
(26) Moore, R. B.; Gauthier, M.; Williams, C. E.; Eisenberg, A. *Macromolecules* **1992**, *25*, 5769–5773.
(27) Starkweather, H. W. *Macromolecules* **1982**, *15*, 320–323.
(28) de Gennes, P. G.; Okumura, K.; Shahinpoor, M.; Kim, K. J. *Europhys. Lett.* **2000**, *50*, 513–518.
(29) Weiland, L. M.; Leo, D. J. *Smart Mater. Struct.* **2004**, *13*, 323–336.
(30) Park, J. K.; Page, K. A.; Hussey, D. S.; Jacobson, D. L.; Arif, M.; Moore, R. B. *Polym. Prepr. (Am. Chem. Soc., Div. Polym. Chem.)* **2008**, *49*, 1006–1007.
(31) Bunn, C. W.; Howells, E. R. *Nature* **1954**, *174*, 549–551.
(32) Chen, Q.; Schmidt-Rohr, K. *Macromol. Chem. Phys.* **2007**, *208*, 2189–2203.

AM8002268